From a discrete to a continuous model of biological cell movement

Stephen Turner,* Jonathan A. Sherratt, and Kevin J. Painter
Centre for Theoretical Modelling in Medicine, Department of Mathematics, Heriot-Watt University, Edinburgh EH14 4AS, Scotland

Nicholas J. Savill
Department of Zoology, Downing Street, Cambridge CB2 3EJ, England
(Received 17 July 2003; published 27 February 2004)

The process by which one may take a discrete model of a biophysical process and construct a continuous model based upon it is of mathematical interest as well as being of practical use. In this work, we take the extended Potts model applied to biological cell movement to its continuous limit. Beginning with a single cell moving in one dimension on a lattice and obeying Potts model rules of movement we develop an expression for the diffusion coefficient of a collection of noninteracting cells which depends explicitly on the Potts model parameters. We show how this coefficient varies when the Potts parameters for cell membrane elasticity and cell-medium adhesion are varied, and perform computer simulations which support our theoretical result. We explain the relationship between the probability of occupancy of lattice points and the density profile in the continuous limit, and extend our analysis by including interactions between the cells. In so doing we are able to develop a set of coupled ordinary differential equations showing the evolution of a density profile in the presence of significant cell-cell adhesion, and show how increases in the strength of this adhesion modulates diffusion. In so doing we develop some insights into how continuous models of physical systems can be based upon discrete models which describe the same system.

DOI: 10.1103/PhysRevE.69.021910 PACS number(s): 87.10.+e

I. INTRODUCTION

The mathematical models which researchers have developed to describe biological phenomena can be divided into three broad categories: continuous (where all variables are considered to be defined at every point in space and time changes continuously), discrete (where space is divided into a lattice of points with the variables defined only at the points and time changes in ''jumps''), and hybrid (a mixture of the previous two). Each of these has advantages and disadvantages depending on the phenomenon under consideration, and on the length scale over which we wish to investigate the phenomenon.

Discrete models of biophysical processes are of use when we are interested in the behavior of individual cells, as well as their interactions with other cells and the medium which surrounds them. Usually, the cells are considered to be points which move on a lattice according to certain rules. These rules can be modified according to the states of neighboring points, such as whether or not they are occupied. Individual based models have found useful application to many physical systems and even simple rules of interaction can give rise to remarkably complex behavior [1]. In particular, individual-based models have found applications in ecology [2], pattern formation [3], tumour growth [4–6], and angiogenesis associated with malignancy [7,8] amongst many others. The application of hybrid models — where cells are modeled as discrete entities with their movements being influenced by continuous spatial fields — has also been found to be a useful approach [9]. A discrete approach to the modeling of cancer invasion developed by two of the authors [10] involves the use of the extended Potts model, which is of particular relevance to the work which we present here.

Continuous models frequently involve the development of a reaction-diffusion equation [11]. These are useful when the length scale over which we wish to investigate the phenomenon is much greater than the diameter of the individual elements composing it. For example, in the biological situation, we would use a continuous model when we are interested in behavior over a length scale much greater than the diameter of one cell. These models have been found to be particularly useful in the study of pattern formation in nature, especially the phenomenon of ''diffusion driven instability'' [12].

Clearly, if we have both a continuous and discrete models of the same phenomenon, we would expect the models to give rise to similar solutions at length scales where their ranges of applicability overlap. Some workers have investigated how one may make this crossover using a variety of techniques: for example, Turchin [13,14] uses the technique of scaling both space and time to develop expressions for the diffusion coefficient which depend explicitly on the individual-based ''hopping'' probabilities on a discrete lattice. Deutsch [15] analyzes (discrete) velocity jump processes to derive (continuous) transport equations applicable to biological systems. An alternative approach involves the development of asymptotic theories which show how different types of equations to describe both diffusion and hyperbolic phenomena can be developed through taking different types of scalings in space and time [16–20].

In this work we have taken the (discrete) Potts model of biological cell movement and shown how it can be used to

*Email address: stephen@ma.hw.ac.uk

 ©2004 The American Physical Society

obtain an expression for the (continuous) diffusion coefficient of a collection of identical noninteracting cells, and present computational results which support our analysis. In Sec. II we first give an overview of the extended Potts model and its applicability to the modeling of biological cell movement. We go on to show how a careful study of the movement of the centers of mass of isolated Potts modeled cells, combined with the taking of suitable limits in space and time, can allow us to develop an expression for the diffusion coefficient of a mass of such cells. This expression (for the diffusion coefficient — a continuous, macroscopic quantity) is explicitly dependent on the (microscopic) Potts model parameters for cell-medium adhesiveness and cell membrane elasticity. In Sec. III we go on to present computer simulation results which are in excellent agreement with this analysis. In Sec. IV we argue that an analogy can be drawn between the probability of occupancy of a lattice point in a discrete model and the local density in the continuous limit. On this basis we introduce interactions between the cells, and develop a set of coupled ordinary differential equations to model the evolution of a density profile composed of cells obeying Potts model rules of movement. We conclude by discussing the insights which this study gives into how discrete models of biophysical processes can be used as a basis for the development of their continuous equivalents.

II. FROM TRANSITION PROBABILITIES TO A DIFFUSION COEFFICIENT

A. Overview of the extended Potts model

The extended Potts model has found application in particular to the problem of differential adhesion driven sorting in a variety of systems [21–26]. Here we give a brief overview of the model, and refer the reader to the previous work of two of the authors for greater detail [10].

We attach to each point (i,j) on a square lattice a label σ_{ij}, and define adjacent points which have the same value of σ to lie within the same cell. Athough there may be many cells present, many of them (if not all) will be of the same type. Hence, we define an additional label τ which defines the type of cell σ_{ij}. Biological cells have receptors on their surfaces associated with adhesiveness [27], and the binding of these receptors with their associated ligands either on a neighboring cell or in the extracellular matrix gives rise to an adhesive energy. We quantify this energy by defining coupling constants J for the energy of interaction between neighboring lattice points with differing values of σ. Hence, the total adhesive energy of the system is given by

$$E_{\mathrm{adh}}=\sum_{ij}\sum_{i'j'}J_{\tau(\sigma_{ij})}J_{\tau(\sigma_{i'j'})}. \tag{1}$$

In addition to adhesiveness, the cells also have a potential energy associated with the elasticity of the cell membrane [28,29], and we define the elastic constant by λ. If the cells have a ''relaxation volume'' V_T (the volume to which they would relax in the abscence of external forces), then the total energy associated with cell membrane elasticity is given by

$$E_{\mathrm{el}}=\sum_{\sigma}\lambda(v_{\sigma}-V_T)^2, \tag{2}$$

where the summation runs over all of the cells in the system and v_{σ} is the instantaneous volume of cell σ. Bringing Eqs. (1) and (2) together we obtain the following term for the total energy of the system:

$$E_{\mathrm{tot}}=\sum_{ij}\sum_{i'j'}J_{\tau(\sigma_{ij})}J_{\tau(\sigma_{i'j'})}+\sum_{\sigma}\lambda(v_{\sigma}-V_T)^2. \tag{3}$$

In evolving the simulated cellular aggregate we use the Monte Carlo method [30]. We consider copying the parameters for one lattice point (i,j) into a neighboring lattice point (i',j'), and work out the total energy change ΔE of the system due to the copy. If this site copy were to result in a reduction in the total energy of the system, then it is accepted. If, however, the energy would be increased then it is accepted with Boltzmann weighted probability

$$p(\sigma_{ij}\rightarrow\sigma_{i'j'})=\begin{cases}1 & \text{if} \quad \Delta H\leqslant 0,\\ e^{-\Delta H/\beta} & \text{if} \quad \Delta H>0,\end{cases} \tag{4}$$

where β is a parameter (analogous to temperature in other physical systems) which quantifies the likelihood of energetically unfavorable events occurring. By repeating these site-copy attempts we are able to track the evolution of the system as it attempts to reduce its total energy. We illustrate in Fig. 1 an example of the evolution of a simulated malignant tumour under the Potts model from the previous work of two of the authors [10].

B. The diffusion coefficient of a Potts modelled cell mass

The diffusion of a collection of noninteracting particles can be studied from two perspectives: we can either observe the behavior of the whole collection and work out its diffusion coefficient by noting the area covered after a given time or we can focus on the behavior of one particle in the collection and work out the behavior of the whole ensemble from a study of the random walk which it performs. If the system is ergodic, then these two approaches will give the same result.

It is our motivation to take the simulated Potts model cells and work out the effective diffusion coefficient of a collection of such cells, so that we may draw a relationship between this coefficient and the Potts model parameters. In our simulations, observing the behavior of a single cell over time is much less computationally intensive than observing the behavior of a large number of cells for a short time. This is because the simulation of a large number of cells requires storing information about each cell in arrays (which may be thousands of elements long) and updating them at each Monte Carlo time step, all of which is very time consuming. Hence — since the ergodic hypothesis states that both approaches will ultimately give the same answer — we concentrate on the behavior of an individual cell, and work out the diffusion coefficient of a collection of identical such cells by studying its movement.

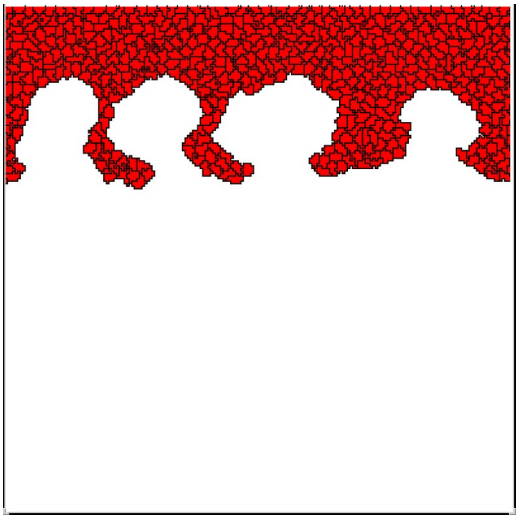

FIG. 1. Showing the characteristic appearance of a simulated tumour. From Ref. [10], where the simulation is described in detail. In this simulation, the cells are experiencing both cell-cell and cell-medium adhesion, and have elastic, deformable membranes. The cell mass is surrounded by extracellular matrix (ECM), and the cells secrete proteolytic enzymes which dissolve it. In so doing they create steep local gradients of ECM protein concentration which the cells are attracted to move up through the process of haptotaxis. In this manner the cells are shown to invade the ECM as long, thick strands of cells — a pattern known as ''fingering,'' which is a hallmark of malignant invasion. Parameters used in the figure (which are described in detail in Ref. [10]): $J_{CC}=3$, $J_{CM}=6$, $k_H=40$, $t=1500$, $n_p=2000$.

Consider a particle moving in one dimension (1D) on a lattice as illustrated in Fig. 2. If one such particle is initially located at point i then there are three things which it can do: move to the right with probability T^+, move to the left with probability T^-, or do nothing with probability $1-(T^+ + T^-)$. Hence, the rate of change of the number of particles at point i is given by [13]

$$\frac{\partial n_i}{\partial t} = T^+_{i-1}(u)n_{i-1} + T^-_{i+1}(u)n_{i+1} - T^-_i(u)n_i - T^+_i(u)n_i, \tag{5}$$

where u is a continuous variable upon which the transition probabilities T^+ and T^- may depend and n_i is the density of particles at point i. If we take the transition probabilites to be equal constants $T^+=T^-=\alpha$, then

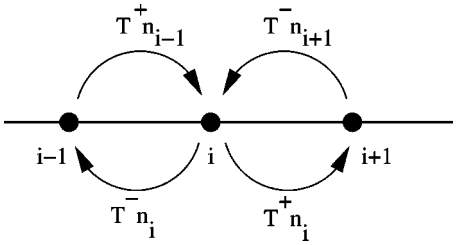

FIG. 2. A schematic diagram of the transition probabilities affecting a particle moving on a 1D lattice.

$$\frac{\partial n_i}{\partial t} = \alpha[n_{i-1} + n_{i+1} - 2n_i]. \tag{6}$$

If we write $n_{i-1}=n(x-h)$, $n_{i+1}=n(x+h)$, where h is the separation between the points, perform Taylor expansions, introduce a scaling $t=\lambda\tau$, and take the limit [13]

$$\lim_{\substack{h\to 0 \\ \lambda\to\infty}} (\lambda h^2) = D \tag{7}$$

then we obtain the diffusion equation

$$\frac{\partial n}{\partial \tau} = \alpha D \frac{\partial^2 n}{\partial x^2}, \tag{8}$$

where we have neglected the $O(h^4)$ and higher terms.

So we see that we can start with knowledge of the discrete transition probabilities T^+ and T^-, and use it to work out the diffusion coefficient. If we relax the assumption $T^+=T^-$, then the resulting diffusion equation becomes nonlinear. Nonlinear diffusion well describes many phenomena in biology [11], but in this work we concentrate on the simple case of linear diffusion.

We note that in the above, and in the derivations that follow, we must regard the diffusion limit as formal since we assume the boundedness of the higher derivatives necessary to validate the limiting procedure. The above method has also been applied to model chemosensitive movement in bacteria, for example, see Othmer and Stevens [31] and Painter, Horstmann, and Othmer [32].

In the Potts model, the cells have finite spatial extent, whereas in the derivation above they are treated as being mathematical points. However, if we concentrate on the movement of the simulated cells' centers of mass (c.m.) then we can use this point-based model. We conduct the following analysis in 1D to make the algebra straightforward, and assume that the results will have qualitative application to higher dimensions. The main reason for this will become evident when we consider the distance moved by the c.m. at each Monte Carlo time step (MCS).

Consider a cell in 1D such as that illustrated in Fig. 3: its c.m. is at the point indicated. In the Potts model simulations, there are four possible changes which can be attempted: an expansion to the right or to the left or a contraction from the right or the left. Each of these changes will have an energy associated with them, and in the simple case of one cell in 1D, the directionality of the movement has no effect on the energy, and ΔE is dependent only on whether an expansion or a contraction is occurring. In the case of there being more than one cell present, this symmetry is lost and directional effects on ΔE have to be included: we consider this higher level of complexity in Sec. IV.

An expansion or contraction of one Potts lattice point results in a movement of the c.m. which is equal to one half of the distance between points on the lattice. Hence, in focussing on the movement of the c.m. we are considering the movement of a point-based particle on a lattice which is twice as fine as the Potts lattice, with two points for every

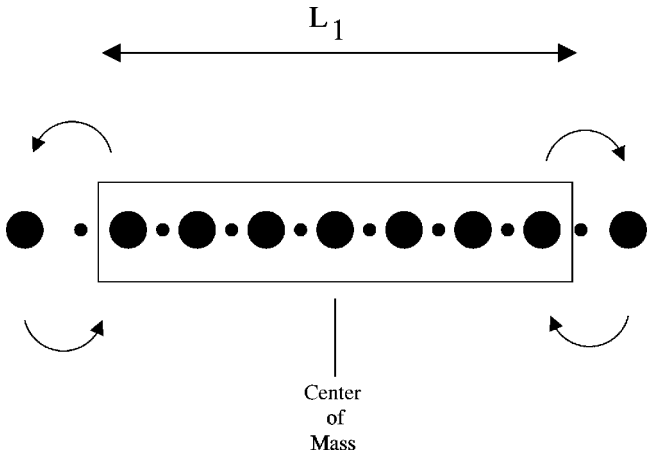

FIG. 3. A diagram of a simulated cell in 1D moving on the Potts lattice (large circles), along with the lattice upon which the cell's center of mass moves during the expansion or contraction of the cell (small circles). The arrows at the extremities of the cell illustrates the four movements which it can make, either by expanding to the right or the left, or shrinking from the right or the left. An expansion or contraction will result in the cell's perimeter increasing or decreasing by a length equal to twice the separation between lattice points (as perimeter is laid down on the top and the bottom of the cell). Following such an expansion or contraction, the cell's center of mass will move a distance equal to one half of the Potts lattice spacing.

Potts lattice point (this also is illustrated in Fig. 3). In 2D and higher, this simplifying assumption is lost, as there is a much greater diversity of possible changes in cell shape at each MCS. Taking this into account makes the analysis far more complex while having little qualitative effect on the results relating the transition probabilities to the Potts parameters and in Sec. III we present computational results which support this assumption.

The energy of a cell at length L has contributions from both the energy of cell-medium adhesiveness and cell membrane elasticity and is given by

$$E_L=[2L+2]J_{\mathrm{CM}}+\lambda[L-L_T]^2. \tag{9}$$

It may be shown that the energy associated with expansion of the cell by one Potts lattice point is given by

$$\Delta E_e=2J_{\mathrm{CM}}+\lambda[1+2(L-L_T)]. \tag{10}$$

whereas that associated with contraction of one lattice point is given by

$$\Delta E_c=-2J_{\mathrm{CM}}+\lambda[1-2(L-L_T)]. \tag{11}$$

We can see from the expression for ΔE_e, if $L<L_T$ it may nevertheless be energetically unfavorable for the cell to expand — even though it is below its target volume L_T — due to the energy expense of laying down perimeter. Similarly, contraction may be unfavorable even though the cell is at a length $L>L_T$. The length which minimizes E_L is given by

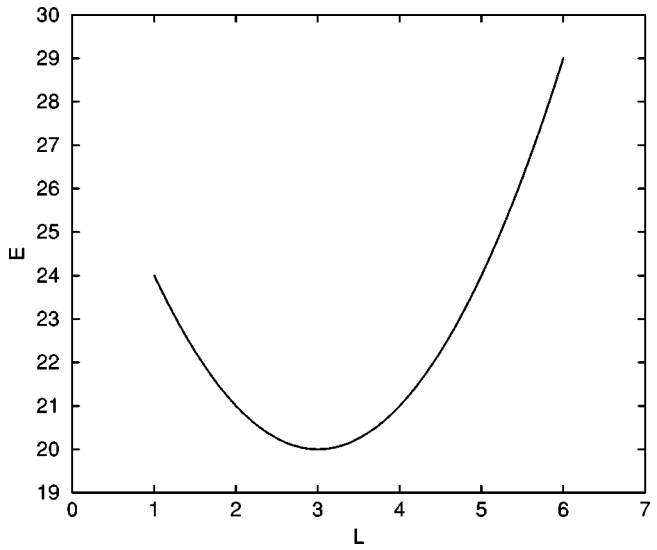

FIG. 4. A sketch of the energy curve for E [given by Eq. (9)] as a function of cell length L for sample values of the Potts parameters. As we can see, the minimum of the energy occurs at a value of L which is not equal to $L_T(=5)$. Note also that, since the energy curve is a quadratic, it is symmetric about $L_{\min}$, and, hence, $E_{(L_{\min}-k)}=E_{(L_{\min}+k)}$, where k is an integer. (Parameters used: $L_T=5$, $\lambda=1$, $J_{\mathrm{CM}}=2$.)

$$L_{\min}=L_T-\frac{J_{\mathrm{CM}}}{\lambda}. \tag{12}$$

Hence, the equilibrium length of the cell is determined by the relative strengths of λ and $J_{\mathrm{c.m.}}$. By substituting Eq. (12) into Eq. (9) we obtain an expression for the minimum energy $E_{\min}$:

$$E_{\min}=2(L_T+1)J_{\mathrm{CM}}-\frac{J_{\mathrm{CM}}^2}{\lambda}. \tag{13}$$

A sketch of E vs L for sample values of L_T, J_{CM} and λ is given in Fig. 4. It tells us that any change in cell length away from $L_{\min}$ results in an increase in its total energy and will be accepted during the Potts model simulations with probability $\exp[-(\Delta E/\beta)]$. Hence, the likelihood of a cell being at length L will be proportional to the difference in energy at this volume E_L and the minimum energy $E_{\min}$:

$$p(L)=\frac{1}{Z}\exp\left(-\frac{(E_L-E_{\min})}{\beta}\right), \tag{14}$$

where $Z=$the partition function, given by

$$Z=\sum_{n=-k}^{k}\exp\left[\frac{1}{\beta}(E_{(L_T+n)}-E_{\min})\right]. \tag{15}$$

Note the parameter k in the summation above. The choice of this is unimportant, provided it is greater than or equal to the maximum deviation from L_T which the cell will attain. Following Potts model rules, the probability of a site copy attempt during which a cell initially at length L_1 expands or contracts to length $L_1\pm1$ will be given by

$$p(L_1 \rightarrow L_1 \pm 1) = \begin{cases} 1 & \text{if} \quad E_{L_1 \pm 1} - E_{L_1} \leqslant 0 \\ \exp^{-(E_{L_1 \pm 1} - E_{L_1})/\beta} & \text{if} \quad E_{L_1 \pm 1} - E_{L_1} > 0. \end{cases} \tag{16}$$

C. Relating energy and Potts modeled movement to diffusion

We can relate the above study to the diffusion coefficient of the cell in the following way. In words: The probability of a cell at position i moving to the right =probability of cell being at length L_1 and moving to the right while at this length + probability of being at length L_2 and moving to the right while at this length + etc. for all possible lengths.

So,

$$T^+ = \sum_{n=-k}^{k} P_{(L_T+n)} P^R_{(L_T+n)}, \tag{17}$$

where $P_{(L_T+n)}$ = probability of being at length L_T+n [given by Eq. (14)] and $P^R_{(L_T+n)}$ = probability of moving to the right while at this length. Similarly,

$$T^- = \sum_{n=-k}^{k} P_{(L_T+n)} P^L_{(L_T+n)}, \tag{18}$$

where the symbols have the same meaning for movements to the left. The cells have to be at *some* size, so in addition the probabilities $P_{(L_T+n)}$ must be normalized to satisfy the condition

$$\sum_{n=-k}^{k} P_{(L_T+n)} = 1. \tag{19}$$

Referring to Fig. 4, since the curve is a quadratic symmetric about $L_{\min}$, it follows that $E_{(L_{\min}-n)} = E_{(L_{\min}+n)}$ where k is an integer. Suppose that the cell is at some length $L = L_T + n$. If a site change is attempted in which the cell would expand in length by one Potts lattice point, then using Eq. (9) it is possible to show that the size of the energy associated with an expansion of one lattice point is given by

$$\Delta E_n = 2J_{\mathrm{CM}} + \lambda(2n+1). \tag{20}$$

If this energy change is negative then the site change will be accepted; conversely, if it is positive it will be accepted with Boltzmann-weighted probability. In the Monte Carlo simulation, there is an equal 50% probability of choosing a point either just inside or just outside of the cell's lateral extremities for copying into its neighbor. Hence, there is an equal chance of expansion or contraction being attempted at each time step. We may therefore conclude that

$$P^R_{(L_T+n)} = P^L_{(L_T+n)} = \frac{1}{4}\left(1 + \exp\left[-\frac{|\Delta E_n|}{\beta}\right]\right), \tag{21}$$

where we have assumed that $P^R_{(L_T+n)} = P^L_{(L_T+n)}$. This assumption is accurate for the single cell case where an expansion to either the right or to the left has the same energy associated with it; however, it breaks down where there is more than one cell present, as the environment in that case has an influence on ΔE. This is discussed in detail later in this chapter.

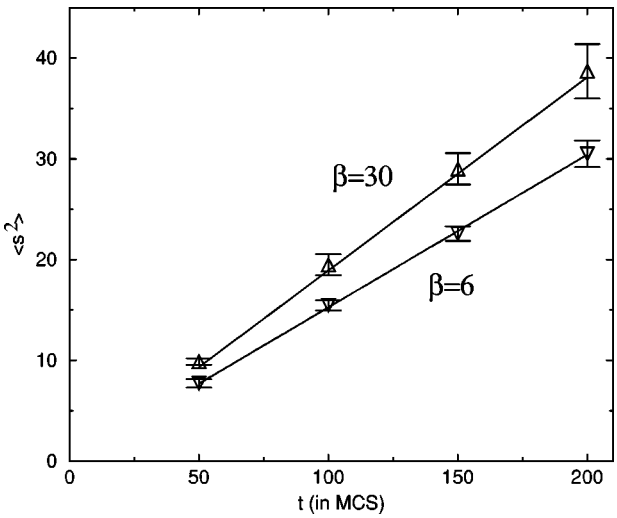

FIG. 5. The relationship between $\overline{\langle s^2 \rangle}$ and time t for two values of β. Lines have been fitted through the data points by least squares fitting. As we can see, the slope of the line is increasing as β is increased. From the Einstein relationship $\langle s^2 \rangle = 2Dt$, this corresponds to an increase in the diffusion coefficient D. (Other parameters: $\lambda = 4$, $J_{\mathrm{CM}} = 2$, $L_T = 5$.)

Substituting Eqs. (14) and (21) into Eq. (17), and recalling the derivation of Eq. (8), we obtain the following expression for the diffusion coefficient of noninteracting Potts modeled cells in terms of the Potts model parameters

$$D = \frac{1}{4Z} \sum_{n=-k}^{k} \exp\left(\frac{E_{\min} - E_{(L_T+n)}}{\beta}\right) \times \left[1 + \exp\left(-\frac{1}{\beta}|2J_{\mathrm{CM}} + \lambda(2n+1)|\right)\right]. \tag{22}$$

In this equation L_T is the length of the cell in the absence of adhesive effects, E_{L_T+n} is the energy at length L_T+n, defined in Eq. 9, where n is an integer, $E_{\min}$ is the minimum energy of the cell, J_{CM} is the cell-medium adhesive energy per unit length, λ is the cell membrane elasticity coefficient, Z is the partition function defined by Eq. (15), and β is a parameter which quantifies the probability of energetically unfavorable events from taking place.

III. COMPUTATIONAL RESULTS

Now that we have a theoretical expression for the diffusion coefficient, we present the results of some Monte Carlo simulations which support it. The mean square distance $\langle s^2 \rangle$ which a single particle will move in time t can be related to the diffusion coefficient of a gas of such particles through the Einstein relation

$$\langle s^2 \rangle = 2Dt. \tag{23}$$

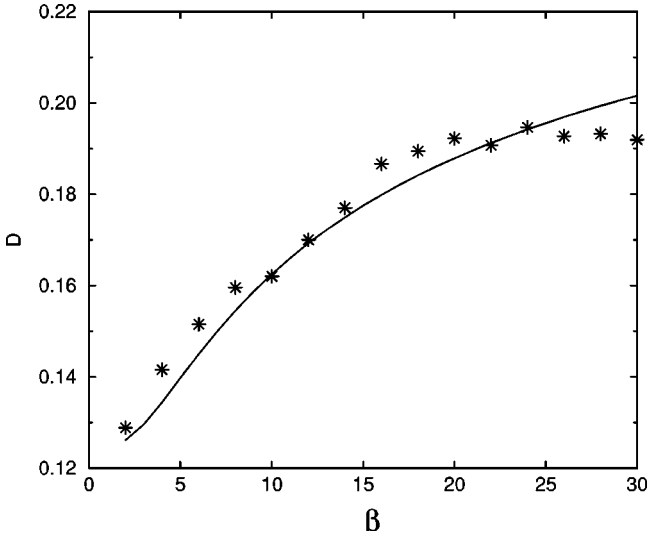

FIG. 6. Diffusion coefficient D vs β. From the lines fitted through the data points in Fig. 5 we work out the diffusion coefficients D. The relationship is initially linear, as we would expect from the Einstein relationship, but at high β, D begins to saturate. This is because, at high β, the Boltzmann weighted probability function tends to 1, and further increases in β have no effect on increasing the motility of the cell. The curve obtained from plotting Eq. (22) as a function of β is overlaid on the data points and, as we can see, there is very good agreement. Note that the saturation effect is stronger in the discrete case: this is because, at high values of β the cells are limited in the number of different shapes which they can take, and begin to fragment. (Parameter values: $\lambda=4$, $J_{\mathrm{CM}}=2$, $L_T=5$.)

Hence, by studying the movement of a single cell in our Potts model simulations, we may work out the diffusion coefficient D for these simulated cells.

We began by running some simulations in 1D for a single cell. We allowed the cell to move for a given number of Monte Carlo time steps (MCS), worked out the mean square distance traveled in that time, repeated this process 500 times, and evaluate the mean squared distance $\langle s^2 \rangle$ for this t. We then repeated this process ten times to get the mean of $\langle s^2 \rangle = \overline{\langle s^2 \rangle}$. The reason for this choice of repetitions was to keep the time required to run the simulations within a reasonable level yet ensuring that the standard deviation of the mean was relatively small ($<7\%$). The results are given in Fig. 5.

From the Einstein relationship, we can work out D from the slope of this set of lines. In Fig. 6 we show the variation of D with the Potts parameter β and have superimposed on the results a curve of Eq. (22) with the same parameter values. As we can see, there is very good agreement between the computational results and the theory. Of course, D is dependent also on the other Potts parameters in Eq. (22), and in Fig. 7 we illustrate the effect of changing the parameters for adhesiveness and membrane elasticity. As we can see, the general shape of the curve is not influenced, but the slope of it is changed in ways which we would expect: increasing the stiffness of the cell membrane reduces its motility, as does increasing J_{CM}.

We mentioned in Sec. II that our results, although obtained from studies of the 1D situation, have qualitative application to higher dimensions. This assumption is supported by our study of the relationship between the mean-squared distance traveled in a given time in 2D, illustrated in Fig. 8: as we can see, there is a linear relationship between $\overline{\langle s^2 \rangle}$ and t, in keeping with the Einstein relationship.

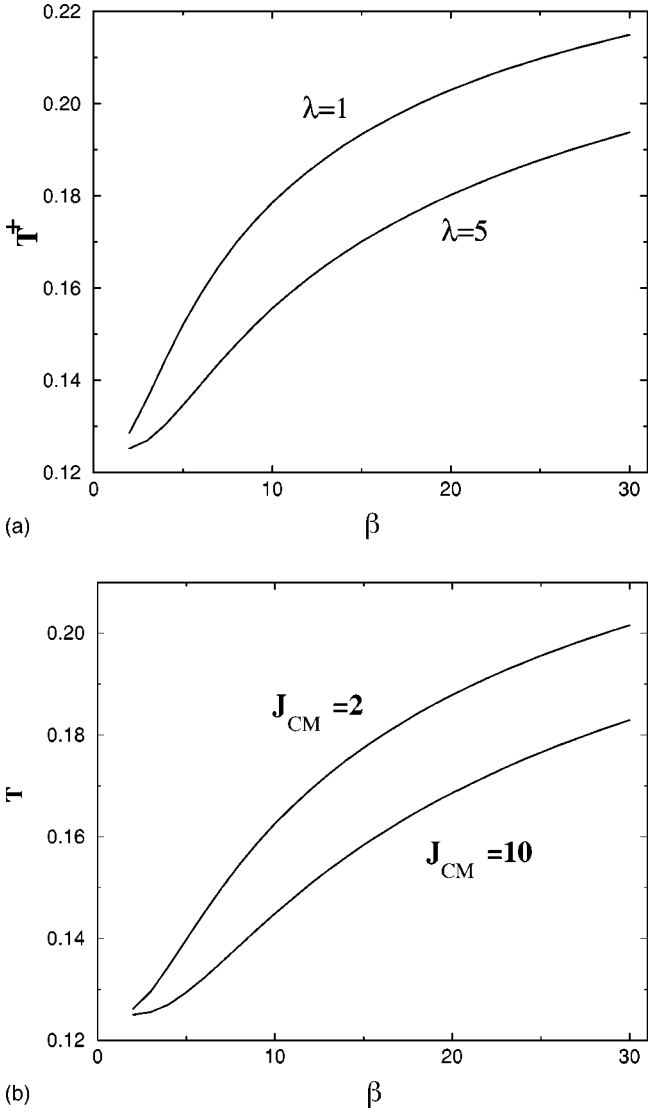

FIG. 7. An illustration of how changes in λ and J_{CM} affect the transition probability as obtained from Eq. (22). Increasing λ has the effect of reducing T^+ across the whole of the range of density (upper graph, with $J_{\mathrm{CM}}=4$). This is as we would expect, as if the membrane is made "stiffer," then it becomes energetically unfavorable for movement of the c.m. to occur. Similarly, if J_{CM} is increased (lower graph, with $\lambda=4$), changes of cell shape which involve an increase in cell perimeter become energetically unfavourable, which reduces the likelihood of such site-swaps occurring, and reduces the motility of the cell.

IV. THE EVOLUTION OF A CONTINUOUS DENSITY PROFILE

As we discussed in Sec. I, continuous models are usually cast in the form of partial differential equations (PDE's).

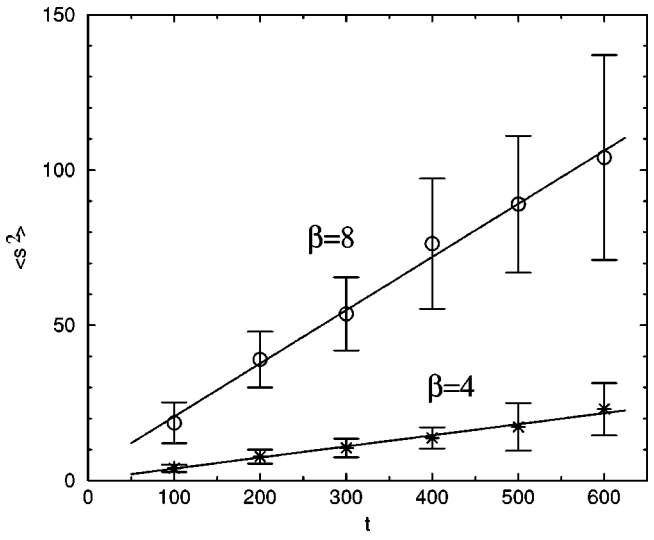

FIG. 8. The relationship between $\langle s^2 \rangle$ and t for the 2D case. As we can see, there is a linear relationship between the two in keeping with the Einstein relationship, and the gradient of the least-squares fitted line increases with increasing β. This supports our assumption that studying the simplified 1D case nevertheless has qualitative application to higher dimensions.

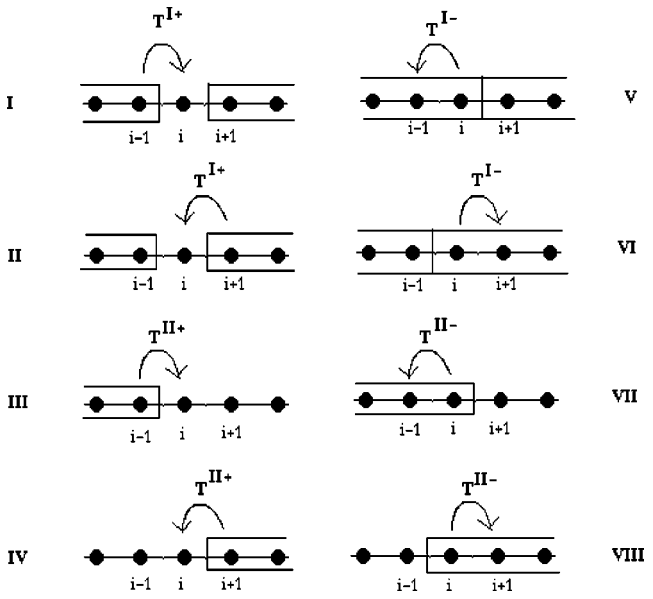

FIG. 9. The eight possibilites for what can happen to lattice point i in the case of multiple cells on a 1D lattice. Scenarios I–IV correspond to the probability of lattice point i being invaded — which corresponds to the number density of cells at point *i increasing* when there are many cells present. Scenarios V–VIII correspond to the cell number density *decreasing*. Note that scenario V is the inverse of scenario I, scenario VI is the inverse of scenario II, and so on.

When we attempt to solve a PDE numerically using a finite difference method, the first step is to discretise space and develop a set of coupled ordinary differential equations (ODE's) to describe the evolution of the dependent variable at each lattice point. In biological situations, usually the coefficients of the PDE are continuous quantities such as the diffusion coefficient. In Sec. II we took a Potts modeled cell and derived a continuous diffusion coefficient for a collection of noninteracting identical cells of this type moving on a lattice following these rules. In this section, we extend this study to include interactions between the cells, and in so doing develop a set of coupled ODE's which describe the evolution of a density profile in which the cells composing it obey Potts model rules of movement.

In our study of cell movement in Sec. II we considered only a single isolated cell moving around the lattice. This had the advantage of making the energy changes associated with movement symmetric in space: the cell's surroundings were isotropically vacant, and the probabilities of movement in every direction were the same (i.e., in 1D $T^+ = T^-$). In the case where there are many cells present, this symmetry is broken as the presence of cells adjacent to the cell of interest influences the likelihood of the cell moving in one direction as opposed to another.

Figure 9 is the many-cell equivalent of Fig. 3, and illustrates the eight possible site-swap events which can happen to lattice point *i*. Each of these has a likelihood of occurrence depending on the probability of the neighboring lattice point being occupied, and on the energy associated with cell-cell contact. Considering the first point, we assume here that an equivalence can be drawn between the probability of occupancy of a lattice point and the continuous number density in this region of space. This equivalence is reasonable if we interpret the physical quantity ''density'' in continuous models as corresponding simply to the probability of a particular point in space being occupied by a cell. Hence, we draw a parallel between the probability of occupancy of a lattice point in the 1D Potts model simulations and the local density in the continuous limit.

Turning now to the influence of energetic changes on the movements of the cells, consider each of the eight possible scenarios illustrated in Fig. 9. Each has an energy associated with it: some of these energies are equal, and some are the same in magnitude but different in sign. If we define the quantity $p_i(t)$ as corresponding to the probability of lattice point i being occupied at time t then the probabilities of each scenario illustrated can be worked out. For example, the probability of configuration I existing in the region of point i at time t is given by (we drop the t's for convenience)

$$p^I = p_{i-1}(1-p_i)p_{i+1}. \tag{24}$$

When lattice point i is invaded through, say, scenario I, where the cell expands into the lattice point from the left, then the invading cell will increase in length. As a first approximation, we assume that the cells do not deviate by much from their target length L_T: this approximation is reasonable from a biological perspective, as in many instances of cell movement, there is not much change in cell volume. Hence, for the invading cell to remain close to L_T there will have to be some contraction at the opposite end of the cell (a distance L_T away) through scenarios VI or VIII. Similarly, if lattice point i is invaded from the right through scenario II then there have to be a contraction at the opposite end of *that*

cell through scenario V or VII, and so on. Since we have assumed that point $i-1$ is occupied, and that the cells are of length L_T, then we can say with certainty that point $i-L_T$ will be occupied. However, point $i-L_T-1$ will be occupied with probability p_{i-L_T-1}. Similarly, since we have assumed that point $i+1$ is definitely occupied, we can say that site $i+L_T$ will also be definitely occupied. However, sites $i-L_T-1$ and $i+L_T+1$ will be occupied with probabilities p_{i-L_T-1} and p_{i+L_T+1}, respectively. Whether or not these sites are occupied will influence the energy change associated with the movement, and, hence, with the probability of it occurring. So, for example, the probability of us having scenario I at point i and scenario VIII to the left is given by

$$p^{\mathrm{I,VIII}}=[p_{i-1}(1-p_i)p_{i+1}](1-p_{i-L_T-1}) \tag{25}$$

and the probability of having scenario II at point i and scenario VII to the right by

$$p^{\mathrm{II,VII}}=[p_{i-1}(1-p_i)p_{i+1}](1-p_{i+L_T+1}). \tag{26}$$

Even though this may be the scenario at a given time, the switch illustrated need not occur as there will be an energy change associated with the cell movement. In this example, one cell-cell bond will form, and two cell-medium bonds will be broken. Hence, if we define $\Delta E^{\alpha}=\Delta E^{\mathrm{I,VIII}}=\Delta E^{\mathrm{II,VII}}=J_{cc}-2J_{CM}$ then the Potts transition probability will be given by

$$T^{\alpha}=T^{\mathrm{II,VII}}=T^{\mathrm{I,VIII}}=\begin{cases}1 & \text{if} \quad \Delta E^{\alpha}\leqslant 0,\\ e^{-\Delta E^{\alpha}/\beta} & \text{if} \quad \Delta E^{\alpha}>0.\end{cases} \tag{27}$$

Hence, the likelihood of site i being invaded through the processes illustrated in scenarios I, VII, and VIII will be given by

$$\frac{dp_i}{dt}=p_{i-1}(1-p_i)p_{i+1}[(1-p_{i-L_T-1})+(1-p_{i+L_T+1})]T^{\alpha}. \tag{28}$$

If we conduct the above analysis for all of the possible ways in which site i could be either invaded or vacated through these mechanisms we can derive a set of coupled ordinary differential equations which describe the evolution of a density profile under these conditions. The details of the derivation of the equations is given in the Appendix. We solved them using a simple Euler method with periodic boundary conditions (we also solved it using zero flux boundary conditions and the results were unchanged). We set as an initial condition a Gaussian profile on a [0,1000] domain, the choice of domain size being determined relative to the size of the individual cells: since $L_T=5$ lattice points, a domain of [0,1000] was considered sufficiently large to allow the system to evolve without boundary effects having a significant effect on the behavior at the center of the profile. The results of evolving the profile under this equation are illustrated in Fig. 10. As we can see, when cell-cell adhesion is weak the system shows a diffusive evolution, as we would expect. However, when cell-cell adhesion is strong, the system shows a changed profile, with slower dispersal.

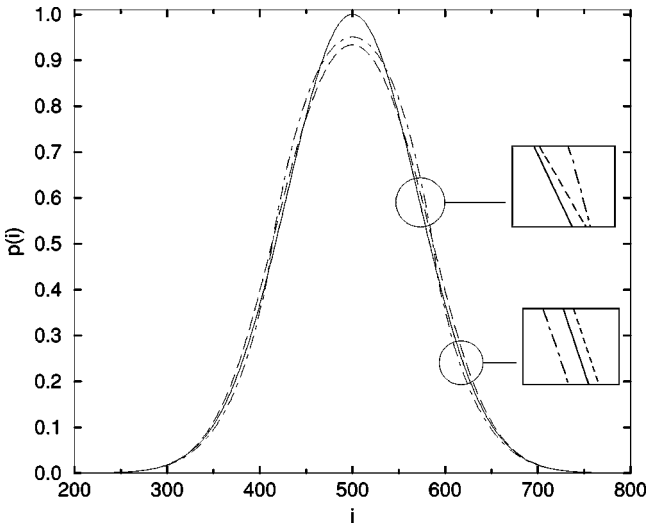

FIG. 10. The evolution of an initially Gaussian profile under Eq. (A1) (solid line: initial condition, dashed line: weak cell-cell adhesion, dot-dashed line: strong cell-cell adhesion). In the case where cell-cell adhesion is weak the evolution is diffusive with movement from high to low regions of density everywhere in space. However, in the case where cell-cell adhesion is strong, the evolution is more complicated: there is movement away from the high density area at the center, but aggregation at regions of intermediate density. ($\lambda=4$, $L_T=5$. Strong adhesion: $J_{\mathrm{CC}}=1$, $J_{\mathrm{CM}}=15$, weak adhesion: $J_{\mathrm{CC}}=15$, $J_{\mathrm{CM}}=1$). The numerical details are as follows: grid size $\Delta x=1$, time step $\Delta t=0.0005$ units, solution plotted after 32 000 iterations. Iterating the solution for longer caused it to become unstable.

Of course, it would be useful if we were able to use this parallel between the probability of occupancy of a lattice point and the density at that point in the continuous limit, to obtain a PDE. In the same way as in our study at the beginning of Sec. II [see Eq. (5)] we could take Eq. (A1), perform Taylor expansions on the p_i, etc., and take appropriate limits in space and time. Due to the number of expansions involved and the additional complexity of including the T^{α}'s, the taking of this limit would be extremely complicated. However, it does allows us to link the previous work on the simple one-cell case with the situation where there is a collection of interacting cells and show the relationship between the two analyses.

V. DISCUSSION

The key point of this work is to make explicit the relationship between a discrete and a continuous model of the same biophysical process, and to illuminate the connection between the macroscopic behavior of a system and the microscopic dynamics of the individual entities which comprise it. In so doing we hope to have given some general insights into how one may take a discrete model and develop expressions for continuous macroscopic quantities based upon it. In particular, through taking suitable limits in space and time in Eqs. (5) – (8) we have shown the connection between the transition probabilities for movement of cells on a discrete

lattice and the corresponding diffusion coefficient for a mass of cells obeying the same microscopic rules. Through a careful study of the movement of the centers of mass of Potts modeled cells, we were able to derive an expression for the diffusion coefficient of a mass of such cells which explictly contained the Potts parameters for cell-cell and cell-medium adhesiveness and cell membrane elasticity. Through invoking the ergodic hypothesis and the Einstein relationship we were able to check this result against computer simulations of the discrete model.

Making clear the relationship between discrete and continuous models of biophysical phenomena is of increasing importance. Recent advances in molecular biology have given us a greatly increased understanding of how microscopic changes in DNA expression can change the characteristics of an individual cell. For example, in the case of cancer, it is known that as a cell progresses along its ''stepwise progression'' to malignancy, it down regulates the expression of cell surface molecules associated with adhesiveness [33]. However, what is of clinical interest — and, therefore, of interest to mathematicians aiming to model these processes — is not the behavior of individual cells, but the macroscopic characteristics of the tumor: how fast it is likely to grow, how deeply it will invade into healthy tissue, the intensity of the radiation which may be needed to treat it (which would in turn be related to the cell density of the tumor), and so on. Similarly, in the diagnosis and treatment of cancer, it is not individual cell behavior which is monitored, but the macroscopic size and appearance of the tumor. So gaining a better understanding of how one may link the insights of molecular biology concerning the behavior of single cells to the macroscopic behavior of a large cellular aggregate is of considerable clinical importance, and mathematics has a useful role to play in illuminating this link.

ACKNOWLEDGMENTS

S.T. was supported by the EPSRC and J.A.S. was supported in part by EPSRC. We thank SHEFC for support (research development grant no. 107).

APPENDIX

Figure 9 illustrates all of the ways in which point i could be invaded or vacated through the movement of Potts modeled cells. If we conduct the analysis described in Sec. IV for all of the possible ways in which the number density at site i could be either increased or decreased through these mechanisms we obtain the following equation:

$$\begin{aligned}\frac{dp_i}{dt} &= p_{i-1}(1-p_i)p_{i+1}[p_{i-L_T-1}T^{\mathrm{I,VI}}+(1-p_{i-L_T-1})T^{\mathrm{I,VIII}}]\\ &+p_{i-1}(1-p_i)p_{i+1}[p_{i+L_T+1}T^{\mathrm{II,V}}+(1-p_{i+L_T+1})T^{\mathrm{II,VII}}]\\ &+p_{i-1}(1-p_i)(1-p_{i+1})[p_{i-L_T-1}T^{\mathrm{III,VI}}+(1-p_{i-L_T-1})T^{\mathrm{III,VIII}}]\\ &+(1-p_{i-1})(1-p_i)p_{i+1}[p_{i+L_T+1}T^{\mathrm{IV,V}}+(1-p_{i+L_T+1})T^{\mathrm{IV,VII}}]\\ &-p_ip_{i+1}[(1-p_{i-L_T})P_{i-L_T-1}T^{\mathrm{V,II}}+(1-p_{i-L_T})(1-p_{i-L_T-1})T^{\mathrm{V,IV}}]\\ &-p_{i-1}p_i[(1-p_{i+L_T})p_{i+L_T+1}T^{\mathrm{VI,I}}+(1-p_{i+L_T})(1-p_{i-L_T+1})T^{\mathrm{VI,III}}]\\ &-p_i(1-p_{i+1})[p_{i-L_T-1}(1-p_{i-L_T})T^{\mathrm{VII,II}}+(1-p_{i-L_T})(1-p_{i-L_T-1})T^{\mathrm{VII,IV}}]\\ &-(1-p_{i-1})p_i[(1-p_{i+L_T})p_{i+L_T+1}T^{\mathrm{VIII,I}}+(1-p_{i+L_T+1})(1-p_{i+L_T})T^{\mathrm{VIII,III}}]. \end{aligned} \tag{A1}$$

This equation can be considerably simplified by making a number of observations. First, we notice that the transition probabilities are symmetric, i.e., $T^{a,b}=T^{b,a}$. Also, we see that there is zero energy change associated with the transitions VIII,IV and VIII,III as the number of cell-cell and cell-medium bonds both before and after the transition is the same. Hence, $\Delta E=0$ and, from Eq. (27), the transition probability is 1. Hence,

$$T^{\mathrm{VII,IV}}=T^{\mathrm{IV,VII}}=1, \tag{A2}$$

$$T^{\mathrm{VIII,III}}=T^{\mathrm{III,VIII}}=1. \tag{A3}$$

Also, we are considering here only directed movement of the cells under the influence of differential adhesion: random movement is not included. For this reason we can safely neglect the transitions where there is no creation or breaking of cell-cell bonds, as these will not influence the evolution of the system due to this process. Hence,

$$T^{\mathrm{V,II}}=T^{II,V}=0, \tag{A4}$$

$$T^{\mathrm{VI,I}}=T^{\mathrm{I,VI}}=0. \tag{A5}$$

Our final simplification is that transitions which have the same energy change associated with them can be set equal. Hence,

$$T^{\mathrm{V,IV}} = T^{\mathrm{VI,III}} = T^{\mathrm{III,VI}} = T^{\mathrm{IV,V}} = 2J_{\mathrm{CM}} - J_{\mathrm{CC}}, \qquad \text{(A6)}$$

$$T^{\mathrm{I,VIII}} = T^{\mathrm{II,VII}} = T^{\mathrm{VII,II}} = T^{\mathrm{VIII,I}} = J_{\mathrm{CC}} - 2J_{\mathrm{CM}}. \qquad \text{(A7)}$$

The numerical solution of Eq. (A1) with these simplifications is illustrated in Fig. 10.

[1] S. Wolfram, Rev. Mod. Phys. **55**, 601 (1983).
[2] L. Berec, Ecol. Modell. **150**, 55 (2002).
[3] J. T. Wootton, Nature (London) **413**, 841 (2001).
[4] S. C. Ferreira, M. L. Martins, and M. J. Vilela, Physica A **261**, 569 (1998).
[5] A. R. Kansal, S. Torquato, E. A. Harsh, G. R. Chiocca, and T. S. Deisboeck, J. Theor. Biol. **203**, 367 (2000).
[6] A. A. Patel, E. T. Gawlinski, S. K. Lemieux, and R. A. Gatenby, J. Theor. Biol. **213**, 315 (2001).
[7] M. Markus, D. Bohm, and M. Schmick, Math. Biosci. **156**, 191 (1999).
[8] A. R. A. Anderson and M. A. J. Chaplain, Bull. Math. Biol. **60**, 857 (1998).
[9] J. C. Dallon and J. A. S. Sherratt, Bull. Math. Biol. **60**, 101 (1998).
[10] S. Turner and J. A. Sherratt, J. Theor. Biol. **216**, 85 (2002).
[11] J. D. Murray, *Mathematical Biology*, 2nd ed. (Springer-Verlag, Berlin, 1993).
[12] A. M. Turing, Philos. Trans. R. Soc. London, Ser. B **237**, 37 (1952).
[13] P. Turchin, J. Anim. Ecol. **58**, 75 (1989).
[14] P. Turchin, *Quantitative Analysis of Movement* (Sinauer Associates, Sunderland, 1998).
[15] A. Deutsch and A. T. Lawniczak, Math. Biosci. **156**, 255 (1999).
[16] T. Hillen and H. G. Othmer, SIAM (Soc. Ind. Appl. Math.) J. Appl. Math. **61**, 751 (2000).
[17] T. Hillen, Math. Models Meth. Appl. Sci. **12**, 1007 (2002).
[18] T. Hillen (unpublished).
[19] M. Lachowicz, Math. Models Meth. Appl. Sci. **12**, 985 (2002).
[20] N. Bellomo and A. Bellouquid (unpublished).
[21] J. A. Glazier and F. Graner, Phys. Rev. E **47**, 2128 (1993).
[22] J. C. M. Mombach, Phys. Rev. E **59**, R3827 (1999).
[23] E. L. Stott, N. F. Britton, J. A. Glazier, and M. Zajaz, Math. Comput. Modell. **30**, 183 (1999).
[24] F. Graner and J. A. Glazier, Phys. Rev. Lett. **69**, 2013 (1992).
[25] D. Drasdo, R. Kree, and J. S. McCaskill, Phys. Rev. E **52**, 6635 (1995).
[26] N. J. Savill and P. Hogeweg, J. Theor. Biol. **184**, 229 (1997).
[27] B. P. L. Wijnhoven, W. N. M. Dinjens, and M. Pignatelli, Br. J. Surg. **87**, 992 (2000).
[28] G. Forgacs, Biol. Bull. **194**, 328 (1998).
[29] J. Guck, R. Ananthakrishnan, C. C. Cunningham, and J. Kas, J. Phys.: Condens. Matter **14**, 4843 (2002).
[30] N. Metropolis and S. Ulam, J. Am. Stat. Assoc. **44**, 335 (1949).
[31] H. G. Othmer and A. Stevens, SIAM (Soc. Ind. Appl. Math.) J. Appl. Math. **57**, 1044 (1997).
[32] D. Painter, K. J. Horstmann, and H. G. Othmer, Appl. Math. Lett. **16**, 375 (2003).
[33] W. G. Stetler-stevenson, S. Aznavoorian, and L. A. Liotta, Annu. Rev. Cell Biol. **9**, 541 (1993).